IET Microwaves, Antennas & Propagation

Research Article

IET Journals
The Institution of Engineering and Technology

Button-shaped radio-frequency identification tag combining three-dimensional and inkjet printing technologies

ISSN 1751-8725
Received on 12th November 2015
Revised on 30th December 2015
Accepted on 19th January 2016
doi: 10.1049/iet-map.2015.0711
www.ietdl.org

Qi Liu[1,2] ✉, Taoran Le[2], Sailing He[1], Manos M. Tentzeris[2]

[1]*Center for Optical and Electromagnetic Research, Zhejiang University, Hangzhou 310027, People's Republic of China*
[2]*School of Electrical and Computer Engineering, Georgia Institute of Technology, Atlanta GA 30308, USA*
✉ *E-mail: lynnchristinalau@hotmail.com*

Abstract: A 'button-shaped' three-dimensional (3D) radio-frequency identification (RFID) tag combining 3D printing and inkjet printing technologies in fabrication for the first time is proposed. The button shape facilitates the tag's integration with clothes for the purposes of identification and access control. The proposed tag features a compact size (radius 15 mm, height 7.5 mm) and a good performance with a measured maximum reading range of 2.1 m (4.0 W equivalent isotropically radiated power) in the RFID Federal Communications Commission band (902–928 MHz). Furthermore, the combination of the 3D printing and inkjet printing technologies reduces the fabrication time and cost.

1 Introduction

Radio-frequency identification (RFID) technology is a remote automatic identification technology, which enables target recognition and relevant data acquisition through RFID. In a typical RFID system, the tag antenna is a vital part and its performance greatly affects the reading range and error rate of the whole RFID system.

RFID's have already found numerous applications in identification authentication, access control and even digital payment [1, 2]. However, in these applications, the RFID tags often have planar structures and function similar to bar-code identification cards. Tags with three-dimensional (3D) structures (such as buttons or accessories on clothes) can easily get integrated with common wearable items and enhance the applicability of RFID systems to Internet of things and smart wearable systems.

3D printing is the technology of building physical objects up layer by layer, based on detailed digital blueprints [3]. Although the previous use of 3D printing technology to RF structures has been relatively limited, the introduction of open-source 3D printing softwares, low-cost 3D printers and advanced and reliable 3D printable materials have led to an increasing number of very promising 3D printed RF devices. The advantages of the 3D printing technology, include time-saving and the capability to fabricate complex structures with arbitrary 3D multimaterial configurations, are typically difficult to realise with traditional fabrication methods.

One of the most common methods of digital printing has been implemented through the use of inkjet printers. Inkjet printing is a direct-write technology by which the design pattern is transferred directly to the substrate. Inkjet printing has been enhanced with the capability of printing new functional materials in the past decade, such as nanoparticle based conductive inks [4–6], leading to its development in printed electronics, such as RFIDs, sensors and antennas [7].

In this paper, we introduce the first 3D RFID tag that has been fabricated by combining 3D and inkjet printing technologies. Unlike traditional RFID tags with planar structures, this tag has a button shape and can be easily used on clothes as a fixed button or a detachable ornament (such as a badge). The advantage of the proposed 3D shape is that it enables its easy 'smart clothes' integration in uniforms as well as in badges of museum visitors and conference participants, as a means for identification authentication and access control, as shown in Fig. 1. The substrate utilised for the 3D printed prototype was made of acrylonitrile butadiene styren (ABS) while the antenna was inkjet printed with silver nanoparticle (SNP) and diamine silver acetate (DSA). With a compact size featuring a radius of 15 mm and a height of 7.5 mm, the printed antenna prototype achieved a simulated maximum gain of −5.6 dB and a maximum measured reading range of 2.1 m with a total transmitted power of 4.0 W equivalent isotropically radiated power.

2 Antenna configuration and physical mechanism

The geometry of the proposed 3D tag antenna is depicted in Fig. 2. The button-shaped substrate is an annular sector with a flat top surface made of ABS ($\varepsilon_r = 2.8$) [8]. The most widely used antenna in RFID tag design is dipole antenna [9], and this is adopted in this design. To accommodate an increased electrical length in a very miniaturised volume, the dipole antenna is designed in an arc configuration and wrapped along the substrate on both top and bottom surfaces. Since the adjusting room for the dipole is limited, an inductively coupled feeding loop is used to perform efficient wide-band conjugate impedance matching between the antenna and the chip without additional matching network [10]. The feeding loop and the middle part of the dipole antenna are placed on the bottom surface, as indicated in black colour in Fig. 2, while the dipole antenna stretches through the side surface to the top surface, as indicated in grey. The dipole and the feeding loop are both inkjet printed with SNP and DSA, an approach that features a high-conductivity value. The feeding loop and the largest part of the dipole are placed on the flat bottom and top planar surfaces to make its high-conductivity inkjet printing. The RFID application specific integrated circuit chip indicated in red colour in Fig. 2 is placed in the middle of the long side of the feeding loop which is away from the dipole.

3 Fabrication process

3.1 3D printing

Most commercial low-cost 3D printers today are using fused deposition modelling [11]. This technology feeds a plastic filament into a heated extruder and then precisely lays down the material [3]. A variety of adjustable options of this technique affects the printing quality. Important properties include layer height,

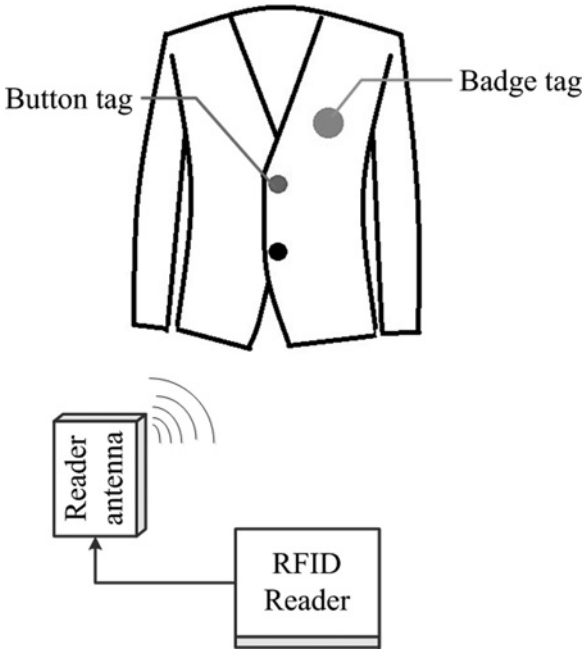

Fig. 1 *Schematic of the 'smart clothes' application of the proposed RFID tag*

perimeters, speed, solid/infill patterns, infill densities, skirt layers, brim width, temperatures and more [12].

All samples were fabricated on the Hyrel [13] System 30 3D printer. This hardware uses a modified version of the Repetier controller software [14], which still uses the common slicing CAD software slic3r [12]. All printing parameters are set in the controller software. The 3D printer was set up to 200 µm layer height, four perimeters and 30 mm/s for all speeds. We printed all layers in solid infill with two skirt layers and a 2 mm brim width.

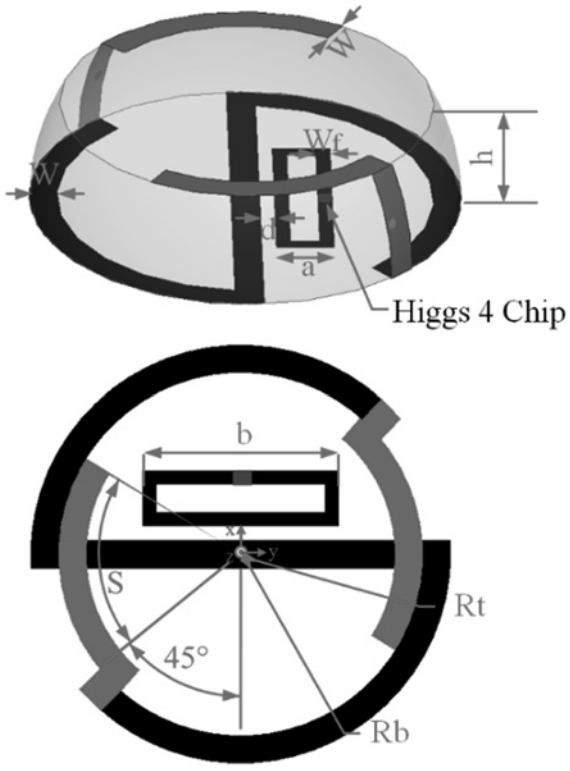

Fig. 2 *Geometry of the proposed RFID tag antenna. R_b = 15 mm, R_t = 13 mm, h = 7.5 mm, W_f = 1 mm, W = 2 mm, a = 14 mm, b = 4 mm, d = 1 mm and S = 65°*

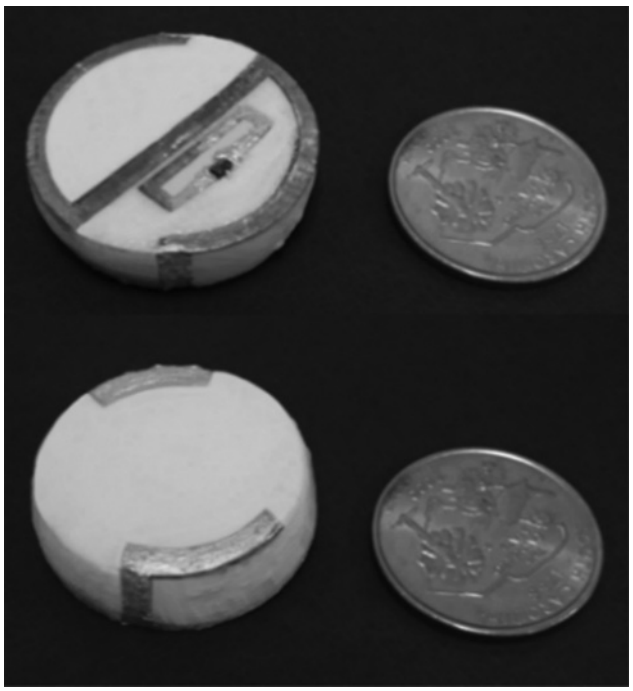

Fig. 3 *Photograph of the fabricated RFID tag prototype: bottom and top views*

The bed temperature is 75°C and extruder temperature of 230°C for the first layer and 225°C for the rest. The fan was running on a full duty cycle.

The finished substrate sample was characterised to evaluate its surface roughness. The surface roughness (Ra) of the bottom surface is the lowest, 3.34 µm, the surface roughness of the top surface is 5.63 µm, while the roughness of the curved side surface is the highest, 10.58 µm. It is still a challenge for us to reduce the roughness of the side surface during the 3D printing process.

3.2 Inkjet printing

There are two critical factors that mainly affect the printing quality: the ink properties and the printing system settings. The most important ink properties include viscosity, density and surface tension. The most crucial settings of the printing system include the nozzle size, droplet volume, droplet generation, the temperature of the jetted and the sintering/curing mechanism performed on the printed structures and so on [7].

In this paper, we have utilised the Dimatix Materials Printer (DMP-2800) series material deposition system [15]. In all prints, the utilised Dimatix 10 pl cartridges were kept at a distance of 0.5 mm from the surface of substrate. The printer head was adjusted to achieve a print resolution of 2540 dpi, which ensures good RF conductivity up to several gigahertz. Four layers of SNP were inkjet printed on the surface of the substrate as base layers. Since some of the nanoparticles sunk into the tiny holes on the substrate surface caused by the 3D printing process and disconnected with other particles, four layers of DSA were added upon SNP layers to reconnect all the SNPs by means of surface tension. In this way, the conductivity got enhanced. After cured in a thermal oven for 1 h at 90°C, the conductivity on the bottom is 3.53×10^7 S/m, while on the top is 2.36×10^7 S/m, due to the fact that the slightly higher surface roughness of the top surface affects the mechanical adhesion of the deposited metal.

4 Experimental results and discussions

A 3D/inkjet-printed tag prototype of the proposed 3D RFID tag is shown in Fig. 3. The circuit works Cw2460 conductive epoxy

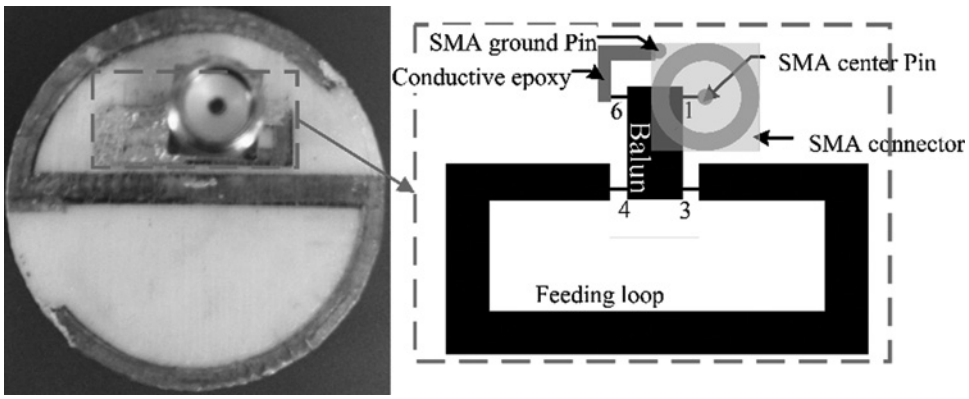

Fig. 4 *Photograph of the fabricated RFID tag prototype: bottom and top views*

with silver colour was applied on the curved side of the button-shaped substrate to realise the side section of the antenna parts on top and bottom surfaces instead of inkjet printing because it is difficult to print on the narrow curved side and the surface roughness of the curved side is relatively high. A Higgs-4 SOT chip with an input impedance of $13.3 - j122\ \Omega$ and a threshold power sensitivity of −18.5 dBm was used in the experiment [16].

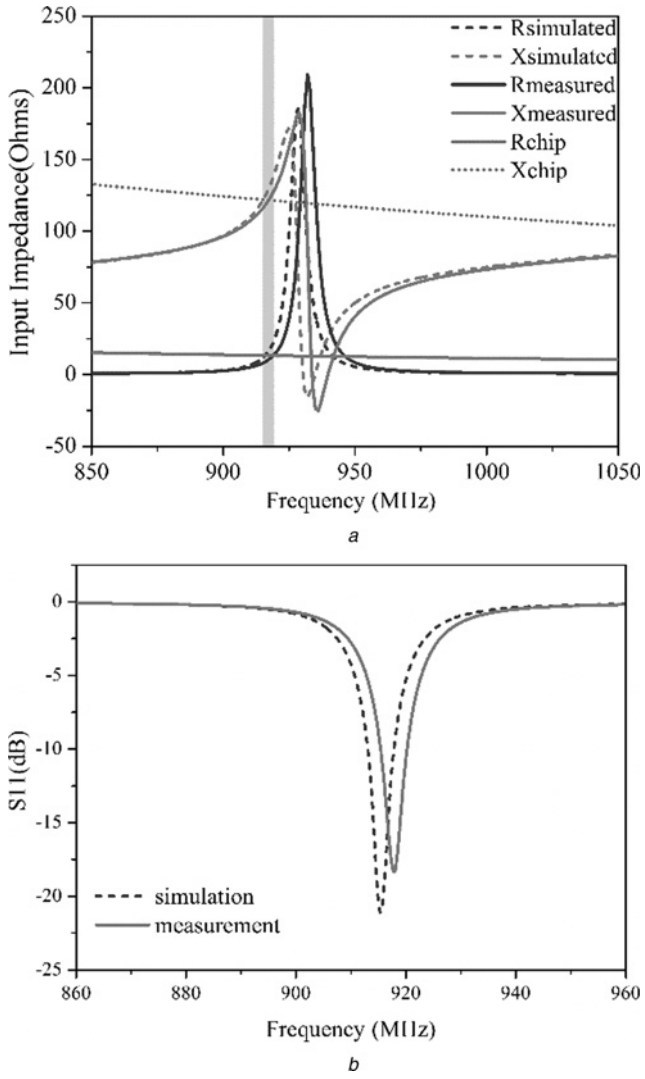

Fig. 5 *Measured and simulated values of*

a Input impedance
b Reflection coefficient *S*11 of the 3D prototype

The antenna prototype was connected to a Johanson 0900BL15C050 900 MHz balun with an SMA connector, as in Fig. 4. The Balun chip is placed between the slots of the feeding loop. The balanced ports of the chip, ports 3 and 4, are connected directly to the feeding loop, while one of the unbalanced ports, port 1, is connected directly to the centre pin of the SMA connector. The other unbalanced port, port 6, and the ground pin of the SMA connector should be connected to each other, but they cannot get touched to each other directly because of the different distances between ports 1 and 6 and between ground and centre pins. Conductive epoxy (circuit works Cw2460; as shown in grey colour in Fig. 4) was added to connect port 6 and ground pin. The antenna was characterised with Rohde & Schwarz ZVA8 vector network analyser. The results of the simulated and measured input impedance are shown in Fig. 5*a*. The simulated impedance is conjugately matched to the chip at about 915 MHz, while the measured impedance is matched at about 920 MHz. The simulated and measured *S*11 results were derived from corresponding input impedance results [17] and presented in Fig. 5*b*, they agree well to each other except the small frequency deviation. The measured resonant frequency of the antenna is 920 MHz, while its simulated value is 915 MHz, a very small difference given the fact that 3D printing introduces tiny gaps and holes in the printed substrate. The 3 dB bandwidth of *S*11 is 908–922 MHz in the simulated result and 910–925 MHz in the measured result, both within the Federal Communications Commission (FCC) band.

The simulated far-field maximum gain is −5.6 dBi, as shown in Fig. 6. This simulated gain has a corresponding reading range of 6.5 m (according to expression 1 in [18]). If longer reading range is needed, we can increase the total size of the antenna to significantly increase the gain and the reading range according to simulation.

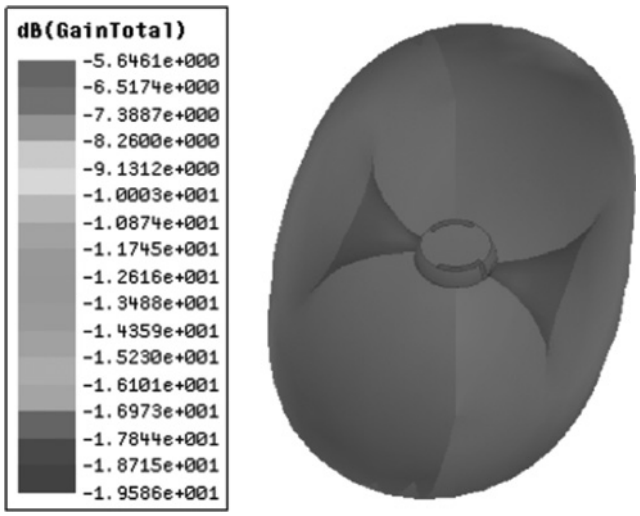

Fig. 6 *Simulated radiation gain pattern of the proposed RFID tag antenna*

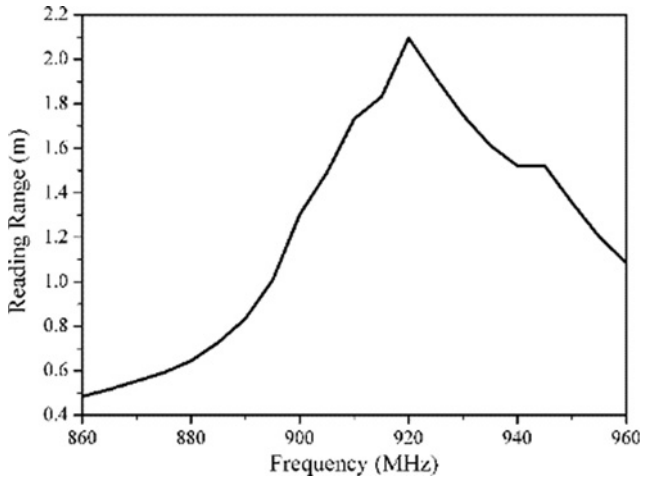

Fig. 7 *Measured maximum reading range*

The reading range of our prototype was measured with Tagformance measurement system [19], shown in Fig. 7, with an output power of 30 dBm and reader antenna gain of 6 dBi, for frequencies over the range from 860 to 960 MHz with a step of 5 MHz. The measured maximum reading range is 2.1 m at 920 MHz, as shown in Fig. 7. The significant decrease in the reading range can be attributed to the experimental lower values of the electric conductivity especially in the side surface, compared with the conductivity of pure silver 6.1×10^7 S/m.

The measured maximum reading range patterns on *XZ* and *XY* planes are shown in Fig. 8. It is obvious that the maximum reading range is in the direction vertical to the button surface, which is the direction we need in practical application. The maximum reading range direction in the *XY*-plane slightly deviates from the axes because of the impact of the adoption of feeding loop.

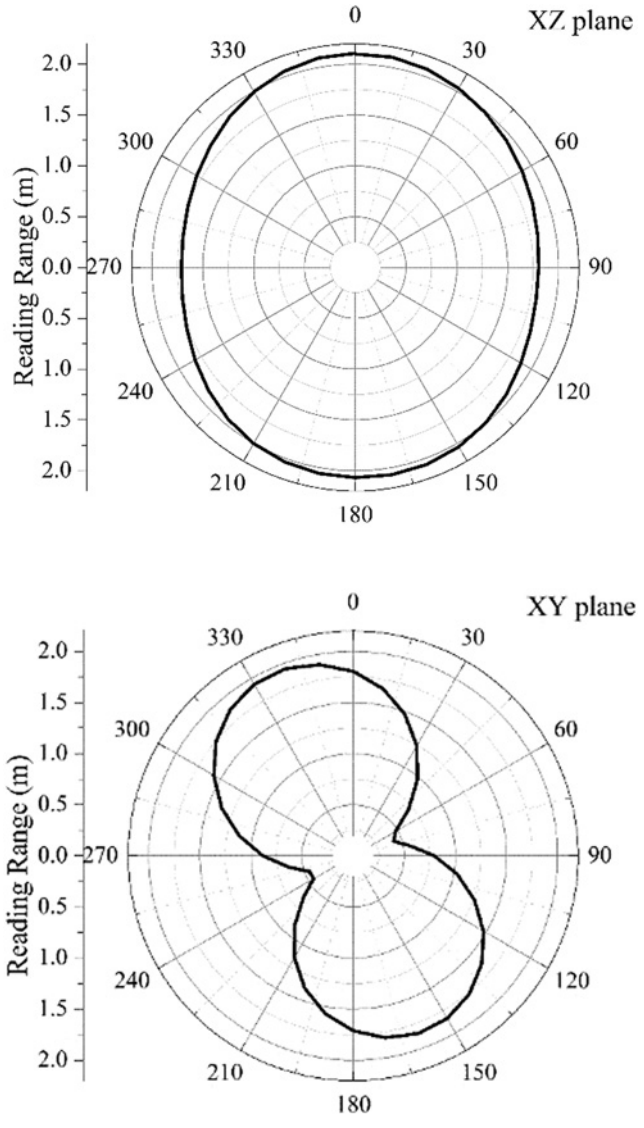

Fig. 8 *Measured maximum reading range patterns on XZ and XY planes*

5 Conclusion

In this paper, we have proposed a 'button-shaped' RFID tag fabricated by the combination of 3D printing and inkjet printing technologies. The button shape makes this tag easy to be attached on numerous wearable platforms, such as clothes, while being used for identification authentication and access control. The tag features a compact size and a good performance with a measured maximum reading range of 2.1 m in the FCC band. The combination of the 3D printing and inkjet printing technologies for the first time in the realisation of truly 3D miniaturised RF structures drastically shortens the fabrication process, while maintaining the accuracy allowing for the easy realisation of virtually unlimited 3D configurations.

6 Acknowledgments

This work was partially supported by the National High Technology Research and Development Program (863 Program) of China (no. 2012AA030402), the National Natural Science Foundation of China (nos. 61178062 and 60990322), the Program of Zhejiang Leading Team of Science and Technology Innovation, Swedish VR grant (# 621-2011-4620), and AOARD.

7 References

1 Ahson, S.A., Ilyas, M.: 'RFID handbook: applications, technology, security, and privacy' (CRC press, 2008)
2 Liu, Q., Yu, Y., He, S.: 'Capacitively loaded, inductively coupled fed loop antenna with an omnidirectional radiation pattern for UHF RFID tags', *IEEE Antennas Wirel. Propag. Lett.*, 2013, **12**, pp. 1161–1164
3 Make: Volume 41, the Ultimate Guide to 3D Printing 2014
4 Le, T., Lakafosis, V., Lin, Z., *et al.*: 'Inkjet-printed graphene-based wireless gas sensor modules'. IEEE Electronic Components and Technology Conf., 2012, pp. 1003–1008
5 Yang, L., Rida, A., Vyas, R., *et al.*: 'RFID tag and RF structures on a paper substrate using inkjet-printing technology', *IEEE Microw. Theory Tech. Trans.*, 2007, **55**, (12), pp. 2894–2901
6 Hester, J.G., Kim, S., Bito, J., *et al.*: 'Additively manufactured nanotechnology and origami-enabled flexible microwave electronics', *Proc. IEEE*, 2015, **103**, (4), pp. 583–606
7 Shaker, G., Safavi-Naeini, S., Sangary, N., *et al.*: 'Inkjet printing of ultrawide band (UWB) antennas on paper-based substrates', *IEEE Antennas Wirel. Propag. Lett.*, 2011, **10**, pp. 111–114
8 Deffenbaugh, P.I., Rumpf, R.C., Church, K.H.: 'Broadband microwave frequency characterization of 3D printed materials', *IEEE Trans. Compon. Packag. Manuf. Technol.*, 2013, **3**, (12), pp. 2147–2155
9 Marrocco, G.: 'The art of UHF RFID antenna design: impedance-matching and size-reduction techniques', *IEEE Antennas Propag. Mag.*, 2008, **50**, (1), pp. 66–79
10 Son, H.-W., Pyo, C.-S.: 'Design of RFID tag antennas using an inductively coupled feed', *Electron. Lett.*, 2005, **41**, (18), pp. 994–996
11 Crump, S.S.: 'Apparatus and method for creating three-dimensional objects'. U.S. Patent 5 121 329, June 1992
12 Hodgson, G.: 'Slic3r Manual'. Available at http://www.manual.slic3r.org/intro/overview, accessed 4 August 2015
13 Hyrel 3D: 'High Reliability 3D printers'. Available at http://www.hyrel3d.com/, accessed 4 August 2015
14 Repetier homepage.: Available at http://www.repetier.com/, accessed 4 August 2015
15 Deposition Products, Fujifilm.: Available at http://www.fujifilmusa.com/products/industrial_inkjet_printheads/deposition-products/index.html, accessed 4 August 2015

16 RFID IC, Alien company.: Available at http://www.alientechnology.com/products/ic/, accessed 4 August 2015
17 Nikitin, P.V., Rao, K.V.S., Lam, S.F., *et al*.: 'Power reflection coefficient analysis for complex impedances in RFID tag design', *IEEE Trans. Microw. Theory Tech.*, 2005, **53**, (9), pp. 2715–2721
18 Rao, K.V.S., Nikitin, P.V., Lam, S.F.: 'Antenna design for UHF RFID tags: a review and a practical application', *IEEE Trans. Antennas Propag.*, 2005, **53**, (12), pp. 3870–3876
19 Tagformance, Voyantic Ltd., Available at https://www.voyantic.com/tagformance/ accessed 4 August 2015